

Orbital-dependent two-band superconductivity in MgB₂

Takashi Yanagisawa^{1,2} and Hajime Shibata¹

¹*Nanoelectronics Research Institute, National Institute of Advanced Industrial Science and Technology (AIST) Tsukuba Central 2, 1-1-1 Umezono, Tsukuba, Ibaraki 305-8568, Japan*

²*Graduate School of Science, Osaka University, Toyonaka 560-0043, Japan*

(Received)

We show that a two-band model with \mathbf{k} -dependent superconducting gaps well describes the transmission and optical conductivity measured for MgB₂ thin films. It is also shown that the two-band anisotropic model consistently describes the specific-heat jump and thermodynamic critical magnetic field H_c . A single-gap anisotropic model is shown to be insufficient to understand consistently optical and thermodynamic behaviors. In our model, the pairing symmetry in each band has an anisotropic characteristic which is determined almost uniquely; the superconducting gap in the σ -band has anisotropy in the ab -plane and the gap in the π -band has a prolate form exhibiting anisotropy in the c -direction. The anisotropy in the σ -band produces rather small effects on the physical properties compared to the anisotropy in the π -band.

Recently discovered superconductor MgB₂ with a relatively high $T_c=39\text{K}$ has attracted much attention in condensed-matter physics.¹ An s -wave superconductivity (SC) was soon established by experiments, e.g., a coherence peak in ¹¹B nuclear relaxation rate² and its exponential dependence at low temperatures.^{3,4} An isotope effect has suggested phonon-mediated s -wave superconductivity.⁵ In contrast to its standard properties, there have been several reports indicating unusual properties of the superconductivity of MgB₂. Several studies reported two different superconducting gaps: a gap much smaller than the expected BCS value and that comparable to the BCS value given by $2\Delta = 3.53k_B T_c$. Their ratio is estimated to be $\Delta_{min}/\Delta_{max} \sim 0.3 - 0.4$ using several experiments.^{3,6-10} It is also reported that the specific-heat jump and the critical magnetic field are reduced compared to the s -wave BCS theory.^{3,10} The other typical characteristic is a strongly anisotropic upper critical field in c -axis-oriented MgB₂ films and single crystals of MgB₂.¹¹⁻¹³

The unusual properties of MgB₂ suggest an anisotropic s -wave superconductivity or a two-band superconductivity. The band structure calculations predicted multi-bands originating from $\sigma(2p_{x,y})$ and $\pi(2p_z)$ bands.¹⁴ In the ARPES measurements performed in single crystals of MgB₂ three distinct dispersions approaching the Fermi energy were reported.¹⁵

There have been several studies on the anisotropy of a superconducting gap.¹⁶⁻²⁰ The two-gap model is shown to consistently describe the specific heat^{18,20} and the upper critical field H_{c2} ¹⁷ with the adoption of the effective mass approach. In this paper, we examine optical properties and thermodynamics to determine the \mathbf{k} -dependence of the gaps. The \mathbf{k} -dependence of two gaps in MgB₂ has never been investigated thus far. We show that the optical transmittance, conductivity, specific-heat jump, and thermodynamic critical field H_c are well de-

scribed by a two-band superconductor model with different anisotropies in \mathbf{k} -space. The symmetry in \mathbf{k} -space is determined almost uniquely according to these experiments. First, we show that the single-gap model is insufficient to understand consistently optical and thermodynamic behaviors. Second, the two-gap model with different symmetries in \mathbf{k} -space is shown to be sufficient to understand optical and thermodynamic properties.

The optical conductivity for anisotropic s -wave SC is investigated and compared with available data for MgB₂. A simple angle-dependent generalization of the Mattis-Bardeen formula²¹ is used to calculate the optical conductivity. The density of states $N(\epsilon) = \epsilon/\sqrt{\epsilon^2 - \Delta^2}$ is generalized to $N(\epsilon) = \langle \text{Re}\epsilon/\sqrt{\epsilon^2 - \Delta_{\mathbf{k}}^2} \rangle_k$, where the bracket indicates the average over the Fermi surface. We employed the following formula at $T=0$:

$$\frac{\sigma_{1s}(\omega)}{\sigma_{1n}} = \frac{1}{\omega} \int_0^\omega dE [N(E)N(\omega - E) - \langle \text{Re} \frac{\Delta_{\mathbf{k}}}{\sqrt{E^2 - \Delta_{\mathbf{k}}^2}} \rangle_k \langle \text{Re} \frac{\Delta_{\mathbf{k}'}}{\sqrt{(\omega - E)^2 - \Delta_{\mathbf{k}'}^2}} \rangle_{k'}]. \quad (1)$$

σ_{2s}/σ_{1n} is similarly generalized. The anisotropic order parameters considered in this paper are:

$$\Delta_{c1}(\mathbf{k}) = \Delta(1 + a\cos(2\theta)), \quad (2)$$

$$\Delta_{c2}(\mathbf{k}) = \Delta(1 - b\cos^2(\theta)), \quad (3)$$

$$\Delta_{ab}(\mathbf{k}) = \Delta(1 + c\cos(6\phi)). \quad (4)$$

Here, θ and ϕ are the angles in the polar coordinate where θ is the polar angle with respect to the c -axis. The parameters a , b and c determine the anisotropy. Δ_{c1} is a prolate form gap for $a > 0$ and is oblate for $a < 0$. Δ_{c2} ($b > 0$) shows the same anisotropy as Δ_{c1} for $a < 0$. Δ_{ab} indicates a cylindrical gap with anisotropy in the a - b

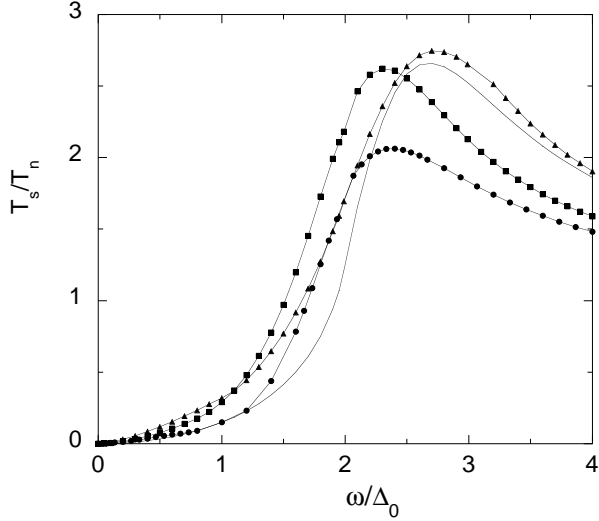


FIG. 1. Transmission T_S/T_N for anisotropic s -wave models. The solid curve without marks is the Mattis-Bardeen result. Squares, triangles and circles are for the prolate, ab-plane anisotropic, and oblate gaps, respectively. The oblate form shows a small increase compared to other types. For the oblate gap, $\Delta_0 = \Delta_{max}$, and for other types, $\Delta_0 = \Delta$.

plane corresponding to the σ band. The integral in eq.(1) is determined numerically by writing the average over the Fermi surface with elliptic functions.

First, we show that the one-band model is insufficient to understand consistently optical and thermodynamic behaviors. In Fig.1 the transmission T_S at $T = 0$ is shown as a function of the frequency ω . The following phenomenological expression for T_S/T_N is employed to determine the transmission curve theoretically,^{23,24}

$$\frac{T_S}{T_N} = \frac{1}{[T_N^{1/2} + (1 - T_N^{1/2})(\sigma_1/\sigma_n)]^2 + [(1 - T_N^{1/2})(\sigma_2/\sigma_n)]^2}, \quad (5)$$

where σ_1 and σ_2 are real and imaginary parts of the optical conductivity, respectively. T_N is determined from the expression for the ratio of the power transmitted with a film to that transmitted without a film given as $T_N = 1/[1 + \sigma_n d Z_0 / (n + 1)]^2$. Here, d is the film thickness, n is the index of refraction of the substrate, and Z_0 is the impedance of free space. We have assigned the following values: $d = 10^{-6}$ cm, $n \approx 3$, $Z_0 = 377\Omega$, and $\sigma_n \approx 8 \times 10^3 \Omega^{-1} \text{cm}^{-1}$. Then we obtain $T_N \simeq 0.014$. The theoretical curves for T_S/T_N are shown in Fig.1; they have peaks near $\omega \sim 2\Delta_0$. For the oblate, its peak shows an increase only twice the normal state value, while the prolate and ab-plane anisotropies show more than twofold increases. The experiments show an approximately 2.5-fold increase²² which supports the prolate or ab-plane anisotropic symmetry. However, the temperature dependence of the ratio H_{c2}^{ab}/H_{c2}^c , which increases as the temperature decreases,¹³ indicates that $\Delta(\mathbf{k})$ has an oblate form instead of a prolate form¹⁶ in contrast to T_S/T_N . It

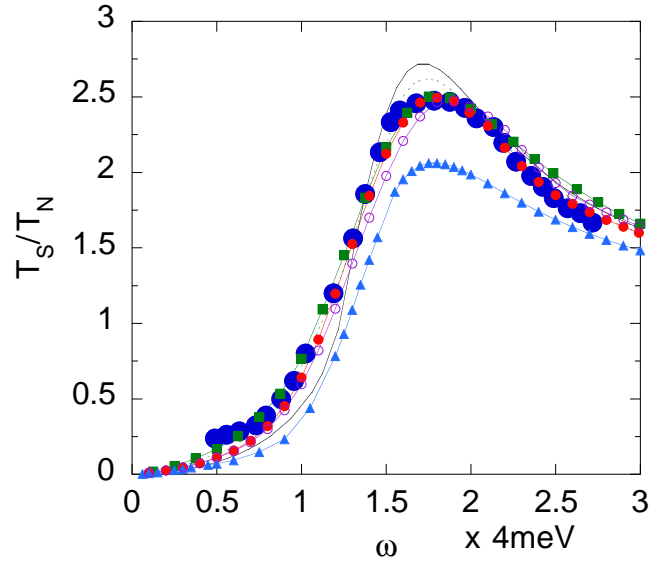


FIG. 2. Transmission T_S/T_N for the two-band model. The data points (large solid circles) are taken from ref.22 at $T = 4\text{K}$. The solid line without marks shows the Mattis-Bardeen result with $2\Delta = 5\text{meV}$. The dotted line is for the single gap of prolate type with $2\Delta_{max} = 9\text{meV}$ and $a = 0.5$. Triangles are for the single-gap model of oblate form with $2\Delta_{max} = 9\text{meV}$ and $a = 0.33$. Others are for the two-band gap model where the ab-plane anisotropic form for the σ -band and the prolate form for the π -band are assumed. The parameters are the following. Solid circles: $2\Delta_{max} = 8.5\text{meV}$ and $c = 0.33$ (σ -band: weight 0.45); $2\Delta_{max} = 6\text{meV}$ and $a = 0.33$ (π -band: weight 0.55). Open circles: $2\Delta_{max} = 9\text{meV}$ and $c = 0.33$ (σ -band: weight 0.45); $2\Delta_{max} = 6\text{meV}$ and $a = 0.33$ (π -band: weight 0.55). Squares: $2\Delta_{max} = 10\text{meV}$ and $c = 0.5$ (σ -band: weight 0.4); $2\Delta_{max} = 7.5\text{meV}$ and $a = 0.5$ (π -band: weight 0.6).

is also difficult to describe the thermodynamic quantities such as the specific-heat jump at $T = T_c$ and the thermodynamic critical magnetic field H_c within the single-gap model consistently. The specific-heat jump at T_c is given by

$$\frac{\Delta C(T_c)}{\gamma_C T_c} = \frac{12}{7\zeta(3)} \frac{\langle z^2 \rangle^2}{\langle z^4 \rangle}, \quad (6)$$

where γ_C is the specific-heat coefficient and z is an anisotropic factor of the gap function. $\langle z^n \rangle$ is the average of z^n over the Fermi surface. The experiments indicate that this value is in the range of $0.76 \sim 0.92$;^{3,10} the fitting parameters must be $a \sim 0.3$, $-a \sim 0.5$ and $c \sim 0.3$ for the prolate, oblate and ab-anisotropic types, respectively. We must assign different values to parameters a and c in order to explain the thermodynamic critical magnetic field H_c . The ratio of $H_c(T = 0)$ to the BCS value is given as

$$H_c(T = 0)^2 / \gamma_C T_c^2 = (6\pi/e^{2\gamma}) \langle z^2 \rangle = 5.94 \langle z^2 \rangle. \quad (7)$$

Thus to be consistent with the experimental results,¹⁰ $\langle z^2 \rangle$ should be less than 1; a should be small, $a \sim 0.07$, for the prolate form, and the ab-plane anisotropic and oblate

forms ($a < 0$) are ruled out since $\langle z^2 \rangle > 1$. In Table I, we summarize the status for the single-gap anisotropic s -wave model applied to MgB₂. As shown here, it is difficult to understand the physical behaviors measured using several experimental methods consistently within the single-gap model.

Here, a two-band model with two different anisotropies is investigated. We assume that the hybridization between σ and π bands is negligible that the optical conductivity is given by

$$\sigma = w_\sigma \sigma_\sigma + w_\pi \sigma_\pi, \quad (8)$$

where σ_σ and σ_π denote the contributions from σ - and π -bands, respectively. The transmission T_S/T_N in Fig.2 shows that the theoretical curve is in good agreement with the experimental curve. The effect of ab -anisotropy for the transmission T_S/T_N is small. The optical conductivity is also described well by the two-band model as shown in Fig.3. We assign the following parameters to the best fit model in Figs.2 and 3. The σ -band has ab -plane anisotropy with $c \approx$ or less than 0.33 and the π -band has the prolate form gap (cigar type) with $a \approx 0.33$. The ratio of the weight of the σ -band to that of the π -band is 0.45/0.55, which agrees with penetration depth⁴ and band structure calculations.²⁵ The ratio of the minimum gap to the and maximum gap is 0.35, which is in

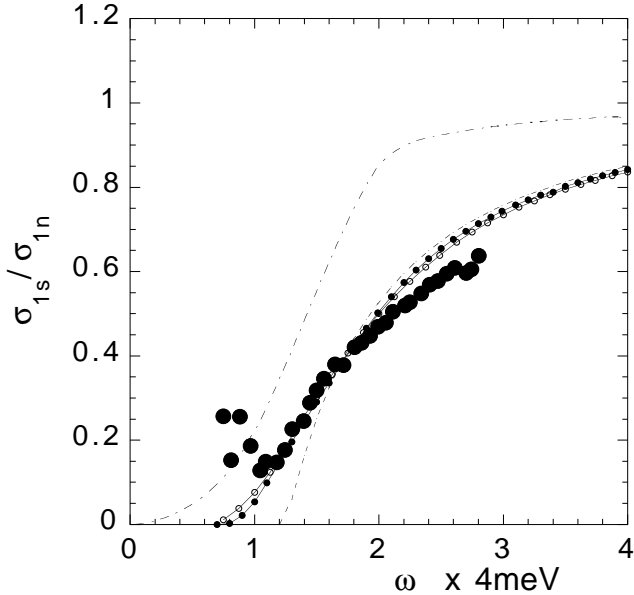


FIG. 3. Real part of the optical conductivity for the two-band anisotropic model. The data points (large solid circles) are taken from ref.22 The parameters for solid circles are $2\Delta_{max} = 8.5\text{meV}$ and $c = 0.33$ (σ -band: weight 0.45); $2\Delta_{max} = 6\text{meV}$ and $a = 0.33$ (π -band: weight 0.55). The parameters for open circles are $2\Delta_{max} = 10\text{meV}$ and $c = 0.5$ (σ -band: weight 0.4); $2\Delta_{max} = 7.5\text{meV}$ and $a = 0.5$ (π -band: weight 0.6). The dashed line indicates the results obtained using the Mattis-Bardeen formula with $2\Delta = 5\text{meV}$. The dash-dotted line denotes the conductivity for the d -wave gap.²³

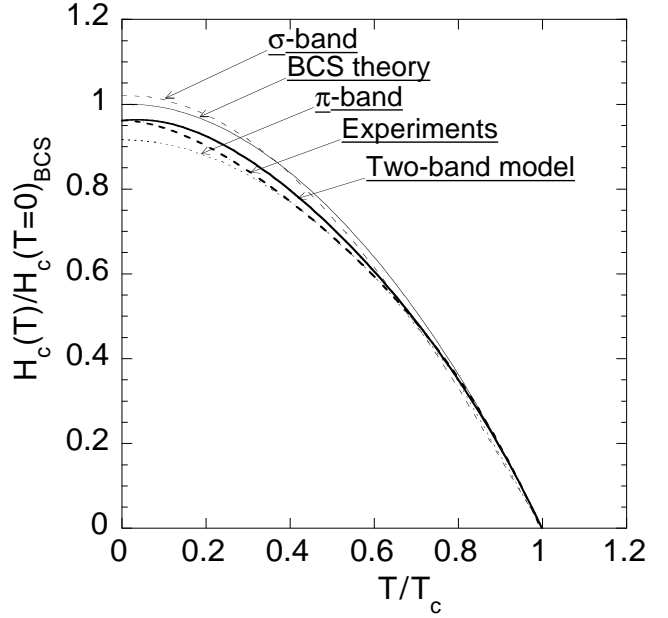


FIG. 4. Thermodynamic critical magnetic field $H_c(T)$ normalized by $H_c(T=0)_{BCS}$. The bold dashed curve indicates data from ref.10 and the bold solid curve indicates those obtained using the present two-band anisotropic model. The thin solid curve indicates the BCS results. The results for the σ -band (ab -plane anisotropic) and the π -band (prolate form) are also shown.

the range of previously reported experimental values.^{6,9} Let us mention here that the two-band isotropic model ($z = 1$) describes inconsistently the observed σ_{1s}/σ_{1n} since a shoulder-like structure is predicted in the two-gap isotropic model if the two gaps have different magnitudes. In Fig.4 the thermodynamic critical magnetic field $H_c(T)$ is shown for the single-band and two-band models with available data.¹⁰ We have simply assumed that the total free energy is given by the sum of two contributions from σ - and π -bands: $\Omega = w_\sigma \Omega_\sigma + w_\pi \Omega_\pi$. The experimental behavior is well explained by the two-band anisotropic model using the same parameters as those for T_S/T_N and σ_{1s}/σ_{1n} . We show several characteristic values obtained from the two-band model in Table II. Results of analyses of H_{c2} and specific heat using the effective mass approach are consistent with those obtained using the two-band model.^{17,18,20} It has been reported that the increasing nature of H_{c2}^{ab}/H_{c2}^c with decreasing temperature is explained by the two-Fermi surface model.¹⁷ The specific-heat coefficient γ in magnetic fields seems consistent with that of the multiband superconductor.^{18,20}

We have examined the transmittance, optical conductivity, specific-heat jump and thermodynamic critical magnetic field H_c of MgB₂ based on the two-band anisotropic s -wave pairing model. We have shown that the two-gap model with different symmetries in \mathbf{k} -space can explain the experimental results consistently.

TABLE I. Anisotropic parameters in the SC gap function used to fit several physical quantities. The upper four rows are for the single-SC gap model and the last row is for the two-band anisotropic model for comparison. The cross indicates that we cannot fit experimental data by the corresponding z factor. Δ in the column H_{c2} indicates that experiments are explained qualitatively but not quantitatively.¹⁶ The big circle show that we can fit the data using the same parameters in the column σ_1 . For the two-gap model the anisotropy parameter in the σ -band can be small since the σ -band anisotropy produces only small effects on physical quantities.

	z	σ_1	T_S/T_N	ΔC	$H_c(0)$	H_{c2}
Cigar-type	$1 + a\cos(2\theta)$	$a \sim 0.5$	~ 0.3	~ 0.3	~ 0.07	\times
Pancake	$1 - a'\cos(2\theta)$	$a' \sim 0.6$	\times	~ 0.5	\times	Δ
Pancake	$1 - b\cos^2(\theta)$	$b \sim 0.75$	\times	~ 0.66	~ 0.08	Δ
In-plane	$1 + c\cos(6\phi)$	$c \sim 0.5$	~ 0.3	~ 0.3	\times	
Two-band	(σ band)	$c \leq 0.3$	\bigcirc	\bigcirc	\bigcirc	
	(π band)	$a \sim 0.3$				

TABLE II. Several physical quantities obtained by the two-band model with $c \sim 0.33$ (σ band) and $a \sim 0.33$ (π band).

	w_σ/w_π	$\Delta_{min}/\Delta_{max}$	$\frac{\Delta C(T_c)}{\Delta C(T_c)_{BCS}}$	$\frac{H_c(0)}{H_c(0)_{BCS}}$
Two-band	0.45/0.55	~ 0.35	~ 0.82	~ 0.95
Exp.	0.45/0.55	0.3 – 0.4	0.76 – 0.92	0.96

- ¹J. Nagamatsu, N. Nakagawa, T. Muranaka, Y. Zenitani and J. Akimitsu: Nature **410** (2001) 63.
- ²H. Kotegawa, K. Ishida, Y. Kitaoka, T. Muranaka and J. Akimitsu: Phys. Rev. Lett. **87** (2001) 127001.
- ³H. D. Yang, J. Y. Lin, H. H. Li, F. H. Hsu, C. J. Liu, S. C. Li, R. C. Yu and C. Q. Jin: Phys. Rev. Lett. **87** (2001) 167003.
- ⁴F. Manzano, A. Carrington, N. E. Hussey, S. Lee, A. Yamamoto and S. Tajima: Phys. Rev. Lett. **88** (2002) 047002.
- ⁵S. L. Bud'ko, G. Lapertot, C. Petrovic, C. E. Cunningham, N. Anderson and P. C. Canfield: Phys. Rev. Lett. **86** (2001) 1877.
- ⁶S. Tsuda, T. Yokoya, T. Kiss, Y. Takano, K. Togano, H. Kito, H. Ihara and S. Shin: Phys. Rev. Lett. **87** (2001) 177006.
- ⁷P. Szabo, P. Samuely, J. Kacmarcik, T. Klein, J. Marcus, D. Fruchart, S. Miraglia, C. Marcenat and A. G. M. Jansen: Phys. Rev. Lett. **87** (2001) 137005.
- ⁸X. K. Chen, M. J. Konstantinovic, J. C. Irwin, D. D. Lawrie and J. P. Frank: Phys. Rev. Lett. **87** (2001) 157002.
- ⁹F. Giubileo, D. Roditchev, W. Sacks, R. Lamy, D.X. Thanh, J. Klein, S. Miraglia, D. Fruchart, J. Marcus and Ph. Monod: Phys. Rev. Lett. **87** (2001) 177008.
- ¹⁰F. Bouquet, R. A. Fisher, N. E. Philips, D. G. Hinks and J. D. Jorgensen: Phys. Rev. Lett. **87** (2001) 047001.
- ¹¹O. F. de Lima, C. A. Cardoso, R. A. Ribeiro, M. A. Avilla and A. A. Coelho: Phys. Rev. **B64** (2001) 144517.
- ¹²M. Xu, H. Kitazawa, Y. Takano, J. Ye, K. Nishida, H. Abe, A. Matsushita, N. Tsuji and G. Kido: Appl. Phys. Lett. **79** (2001) 2779.
- ¹³M. Angst, R. Puzniak, A. Wisniewski, J. Jun, S. M. Kazakov, J. Karpinski, J. Roos and H. Keller: Phys. Rev. Lett. **88** (2002) 167004.
- ¹⁴J. Kortus, I. I. Mazin, K. D. Belashchenko, V. P. Antropov and L. L. Boyer: Phys. Rev. Lett. **86** (2001) 4656.
- ¹⁵H. Uchiyama, K. M. Shen, S. Lee, A. Damascelli, D. H. Lu, D. L. Feng, Z. X. Shen, and S. Tajima: Phys. Rev. Lett. **88** (2002) 157002.
- ¹⁶S. Haas and K. Maki: Phys. Rev. **B65** (2001) 020502.
- ¹⁷P. Miranovic, K. Machida and V.G. Kogan: J. Phys. Soc. Jpn. **72** (2003) 221.
- ¹⁸N. Nakai, M. Ichioka and K. Machida: J. Phys. Soc. Jpn. **71** (2002) 23.
- ¹⁹L. Tewordt and D. Fay: Phys. Rev. Lett. **89** (2002) 137003.
- ²⁰F. Bouquet, Y. Wang, I. Sheikin, T. Plackowski, A. Junod, S. Lee and S. Tajima: Phys. Rev. Lett. **89** (2002) 257001.
- ²¹D. C. Mattis and J. Bardeen: Phys. Rev. **111**, 412 (1958).
- ²²R. A. Kaindl, M. A. Carnahan, J. Orenstein and D. S. Chemla: Phys. Rev. Lett. **88** (2002) 027003.
- ²³T. Yanagisawa, S. Koikegami, H. Shibata, S. Kimura, S. Kashiwaya, A. Sawa, N. Matsubara and K. Takita: J. Phys. Soc. Jpn. **70** (2001) 2833.
- ²⁴R. E. Glover and M. Tinkham: Phys. Rev. **108** (1957) 243.
- ²⁵K. D. Belashchenko, M. van Schilfgaarde and V. P. Antropov: Phys. Rev. **B64** (2001) 092503.